

## Fission time-scale from the measurement of pre-scission light particles and $\gamma$ -ray multiplicities

K RAMACHANDRAN<sup>1,\*</sup>, A CHATTERJEE<sup>1</sup>, A NAVIN<sup>1,2</sup>, K MAHATA<sup>1</sup>,  
A SHRIVASTAVA<sup>1</sup>, V TRIPATHI<sup>1,3</sup>, S KAILAS<sup>1</sup>, V NANAL<sup>4</sup>,  
R G PILLAY<sup>4</sup>, A SAXENA<sup>1</sup>, R G THOMAS<sup>1</sup>, D R CHAKRABARTY<sup>1</sup>,  
V M DATAR<sup>1</sup>, SURESH KUMAR<sup>1</sup> and P K SAHU<sup>1</sup>

<sup>1</sup>Nuclear Physics Division, Bhabha Atomic Research Centre, Mumbai 400 085, India

<sup>2</sup>Permanent address: GANIL, Bd. Henri Becquerel, BP 55027, Cedex-5, Caen, France

<sup>3</sup>Present address: Department of Physics, Florida State University, Tallahassee, Florida 32306, USA

<sup>4</sup>Department of Nuclear and Atomic Physics, Tata Institute of Fundamental Research, Colaba, Mumbai 400 005, India

\*Corresponding author. E-mail: kram@barc.gov.in

DOI: 10.1007/s12043-015-1048-y; ePublication: 19 July 2015

**Abstract.** An overview of the experimental result on simultaneous measurement of pre-scission neutron, proton,  $\alpha$ -particle and GDR  $\gamma$ -ray multiplicities for the reaction  $^{28}\text{Si}+^{175}\text{Lu}$  at 159 MeV using the BARC–TIFR Pelletron–LINAC accelerator facility is given. The data were analysed using deformation-dependent particle transmission coefficients, binding energies and level densities which are incorporated in the code JOANNE2 to extract fission time-scales and mean deformation of the saddle-to-scission emitter. The neutron, light charged particle and GDR  $\gamma$ -ray multiplicity data could be explained consistently. The emission of neutrons seems to be favoured towards larger deformation as compared to charged particles. The pre-saddle time-scale is deduced as  $(0-2) \times 10^{-21}$  s whereas the saddle-to-scission time-scale is  $(36-39) \times 10^{-21}$  s. The total fission time-scale is deduced as  $(36-41) \times 10^{-21}$  s.

**Keywords.** Fusion–fission; fission time-scale; pre-scission time; saddle-to-scission time; pre-scission neutron multiplicity; pre-scission proton multiplicity; pre-scission  $\alpha$ -particle multiplicity; pre-scission GDR  $\gamma$ -ray multiplicity.

PACS Nos 25.70.Jj; 25.85.Ge

### 1. Introduction

Nuclear fission is a unique process in which the shape of a nearly equilibrated system evolves continuously until it splits into two fragments. It is found that the evolution takes more time than the prediction of statistical model calculations due to the viscous nature

of the nuclear medium [1–13]. The time taken for a compound nucleus (CN) to fission depends upon both the statistical and the dynamical properties of the fissioning system.

Fission lifetime can be measured using direct methods like crystal blocking technique [14], K-vacancy production [15] and indirect methods like neutron clock [1,12], light charged particle clock [1,16], GDR clock [2,10], evaporation residues (ER) cross-section [2,17,18] and fission probabilities [19,20]. Early measurements [10,12] using the neutron and GDR clocks showed that the fission time-scales were much larger than those predicted by the standard statistical model. However, results from the measurements of pre-scission light charged particles [21] could be understood in terms of the usual statistical model, without introducing any delay in the fission process. Progress was made in resolving this puzzling feature [11,16] by incorporating deformation-dependent particle binding energies and transmission coefficients. The direct measurements of fission time-scales like crystal blocking technique [14,22–24] and measurement of K-vacancy production [15,25] are sensitive to long lifetimes in the range of  $\sim 10^{-18}$  s–  $\sim 10^{-16}$  s and hence can only probe a part of the fission time distribution. These measurements have consistently shown fission time-scales one or two order larger than the other indirect methods [14]. Fregeau *et al* [15] have deduced a minimum mean fission time of  $2.5 \times 10^{-18}$  s for  $Z = 120$  nuclei from a recent measurement on X-ray multiplicity. Such large fission time-scales were not observed using indirect methods.

These discrepancies could be due to either the experimental uncertainties or the model analysis, which makes several assumptions and simplifications. A simultaneous measurement of most number of observables could be useful in eliminating the possible systematic uncertainties. Also a simultaneous reproduction of all the experimental data using a single model could be useful in understanding these discrepancies. Currently, no such model is available.

Saxena *et al* [7] made a simultaneous measurement of pre-fission neutron and  $\alpha$ -particle multiplicities for 340 MeV  $^{28}\text{Si}$  on  $^{232}\text{Th}$ . The fission time-scale deduced from the neutron data was  $50_{-30}^{+70}$  zs, while the  $\alpha$  data were inconsistent with this. Schmitt *et al* measured the pre-fission neutron and GDR  $\gamma$ -ray multiplicities simultaneously [6] and obtained fission time-scales which differed up to a factor of 2. These discrepancies could be due to the inadequate modelling of fission dynamics. Fission being a dynamical process, a dynamical model like the Langevin dynamics coupled with statistical evaporation of light particles and photons will be useful. Even though the calculations are challenging, there are some progress in this direction [26,27].

We have measured the pre-scission neutron, proton,  $\alpha$ -particle and GDR  $\gamma$ -ray multiplicities simultaneously for  $^{28}\text{Si} + ^{175}\text{Lu}$  at 159 MeV. The fission time-scales were extracted using the statistical model code JOANNE2 [11] which includes deformation effects. In this study, a short summary of the results from neutron, proton and  $\alpha$ -particle multiplicity data [1] along with a detailed discussion on the GDR  $\gamma$ -ray multiplicity will be given.

## 2. Results from neutron, proton and $\alpha$ -particle clock

A pulsed 159 MeV  $^{28}\text{Si}$  beam was obtained from the BARC–TIFR Pelletron–LINAC accelerator facility. The target was a 1.5 mg/cm<sup>2</sup> self-supporting foil of  $^{175}\text{Lu}$ . The experimental configuration is shown in figure 1. Further details about the fission, neutron and

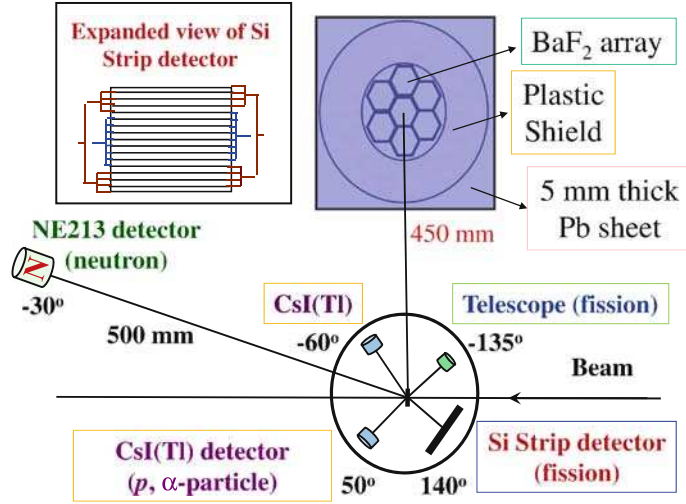
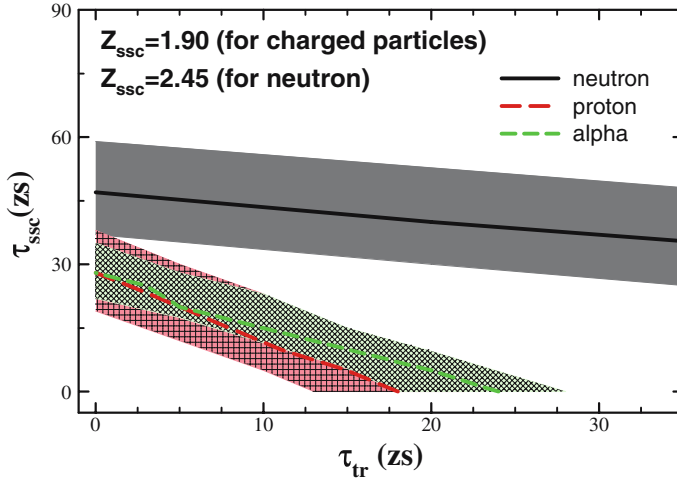


Figure 1. Schematic representation of the experimental set-up (see text).

light particle detectors used along with the data analysis can be found in [1]. In summary, after the energy and efficiency calibration of the neutron spectra from NE213 liquid scintillator detector, energy calibration of the proton and  $\alpha$ -particle spectra from CsI(Tl) detector, in coincidence with fission fragments in the fission detectors, the spectra were normalized with single fission to get the multiplicity spectra. Proper background subtractions were also done. The multiplicity spectra were fitted with the moving source model to extract the pre- and post-scission multiplicity.

Statistical model calculations using the code JOANNE2 were performed to reproduce the experimental pre-scission neutron, proton and  $\alpha$ -particle multiplicities. The code incorporates the effects of deformation dependence of particle binding energies and particle transmission coefficients [11,16] on fission time-scales. Deformation-dependent level densities [28] have been used in these calculations. Pre-scission emission is assumed to take place from two points in the deformation space, corresponding to mean pre-saddle deformation ( $Z_{tr}$ ) and mean saddle-to-scission deformation ( $Z_{ssc}$ ). Pre-saddle emission takes place over the region from equilibrium to saddle. For this purpose, mean deformation of the pre-saddle emitter was taken as  $Z_{tr} = 1.31$  (in units of the diameter of the spherical system).  $Z_{ssc}$  along with mean pre-saddle time ( $\tau_{tr}$ ) and mean saddle-to-scission time ( $\tau_{ssc}$ ) were varied. The level density parameter  $a_n$  for spherical compound nucleus,  $a_{ssc}$  for each  $Z_{ssc}$  and  $a_f/a_n$  were calculated [28]. Fission barriers of 1.10 times the rotating finite range model (RFRM) value were used [29,30].

The combination of  $\tau_{tr}$  and  $\tau_{ssc}$  values required to explain  $\nu_{pre}$ ,  $\pi_{pre}$  and  $\alpha_{pre}$  independently were calculated for  $Z_{ssc} = 1.9, 2.17$  and  $2.45$ . For  $Z_{ssc} = 2.17$ , a large total fission time ( $\tau_{tot} \sim 125$  zs) was required to explain  $\nu_{pre}$ . However, to explain  $\pi_{pre}$  and  $\alpha_{pre}$ , a smaller time-scale of  $\tau_{tot} \sim 40$  zs was sufficient. With other  $Z_{ssc}$  values also there was no unique set of  $\tau_{tr}$  and  $\tau_{ssc}$  which could explain  $\nu_{pre}$ ,  $\pi_{pre}$  and  $\alpha_{pre}$  simultaneously. A consistent interpretation was obtained by considering neutrons and charged particles emitted from different deformations. This is shown in figure 2 where the correlated plots are made with  $Z_{ssc} = 2.45$  for neutrons and 1.90 for charged particles. Here, an overlapping region



**Figure 2.** Combinations of  $\tau_{tr}$  and  $\tau_{ssc}$  required to reproduce experimental  $\nu_{pre}$ ,  $\pi_{pre}$  and  $\alpha_{pre}$  data [1] are shown as continuous, long and medium dashed line, respectively. The shaded regions correspond to experimental errors.

was obtained for the fission lifetimes with  $\tau_{ssc} = (36-39)$  zs and  $\tau_{tr} = (0-2)$  zs with a total lifetime  $\tau_{tot} = (36-41)$  zs.

This implied that the emission of neutrons takes place predominantly from larger  $Z_{ssc}$  ( $\sim 2.4$ ) while light charged particles were probably emitted from the deformation region  $Z_{ssc} < 2.0$ . Larger value of  $Z_{ssc}$  decreases the neutron binding energy [11] reduces the value of  $\tau_{ssc}$  required to explain  $\nu_{pre}$ . For proton and  $\alpha$  emission, the combination of binding energy and emission barrier decides whether  $\tau_{ssc}$  increases or decreases with  $Z_{ssc}$ . The result also indicated that the pre-saddle time is less than 2 zs which is in agreement with the conclusion of recent fission time-scale measurements using the fission probability probe [19,20].

### 3. Results from GDR $\gamma$ -ray multiplicity

In addition to the fission, neutron and light charged particle detectors, an array of seven BaF<sub>2</sub> detectors in a hexagonal close-packed geometry and having a plastic anticoincidence shield [31] was used to detect high-energy  $\gamma$ -rays. The array was placed at a distance of 45 cm from the target and at 90° to the beam direction. Each BaF<sub>2</sub> detector had a length of 20 cm and a hexagonal cross-section with a face-to-face distance of 6 cm. The annular plastic detector was a cylinder of 5 cm thickness and 40 cm length which was used to reject the cosmic ray background. The excellent beam timing of  $\sim 800$  ps allowed a clean  $n-\gamma$  separation using TOF technique. Shape analysis of the BaF<sub>2</sub> pulse was used to reject pile-up events. Pulse shape analysis was done by sending summed energy signal to two QDCs, with 2  $\mu$ s and 200 ns gates, the outputs (parameters EL and ES, respectively) of which were recorded event-by-event. The ratio of ES to EL for events with no pile-up is different from those with pile-up. By introducing an appropriate gate on this ratio in the offline analysis, pile-up events were rejected. The BaF<sub>2</sub> detectors were calibrated using

the 4.44 and 6.13 MeV  $\gamma$ -rays from  $^{241}\text{Am}-^9\text{Be}$  and  $^{238}\text{Pu}-^{13}\text{C}$  sources, respectively. The response function of the detector for various  $\gamma$  energies required to convolute a theoretical spectrum before comparison with the experimental spectrum was generated using the simulation code, electron gamma shower (EGS4) [32].

Fission-gated  $\gamma$ -ray spectra were also obtained after correcting for random coincidences. Figure 3 shows the normalized GDR  $\gamma$ -ray multiplicity spectra in coincidence with the strip detector after convoluting with the response function.

Similar to the neutron and light charged particle spectra, the GDR  $\gamma$ -ray spectrum also has components mainly from the two fission fragments and compound nucleus. In this case it is not possible to fit the measured spectra directly because of the complications arising from the detector response function. Hence, to separate the components of the experimental GDR  $\gamma$ -ray multiplicity spectra, all the three components were calculated using the statistical model code JOANNE2 suitably modified to include the GDR emission. After applying Doppler correction, these spectra were folded with the response function of the detector. Correction for absorption in the lead sheet kept in front of the  $\text{BaF}_2$  array was also done. The folded spectra were added and compared with the experimental spectra. Being perpendicular to the beam axis, the emission from CN (pre-scission component) does not have any Doppler correction. Doppler correction for the detected fission fragments were carried out for an average relative angle between the  $\text{BaF}_2$  detector array and the Si strip detector. For the complementary fission fragment a mean mass and a mean total kinetic energy for the fission fragments were assumed while calculating its angle using the TKE predicted by Viola systematics and two-body kinematics.

Having performed a simultaneous measurement, a simultaneous analysis using a single code JOANNE2 was attempted. The original code did not have the GDR  $\gamma$  as a competing

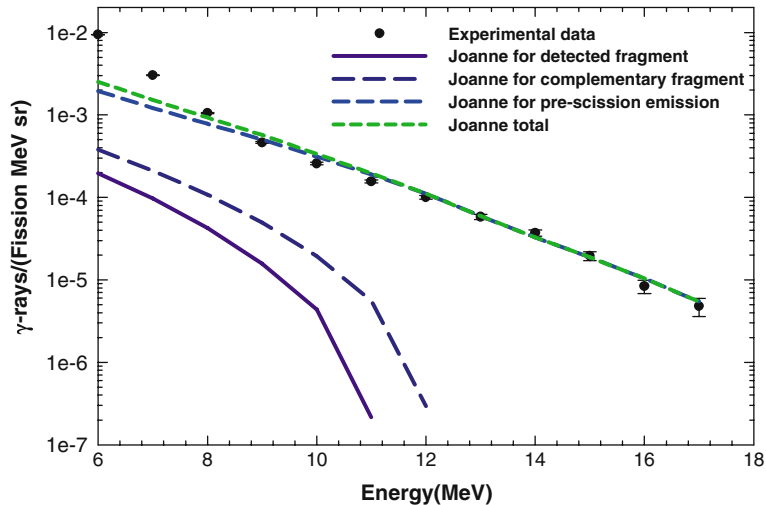


**Figure 3.** GDR  $\gamma$ -ray multiplicity spectra [2] ( $\bullet$ ) along with JOANNE2 output for  $Z_{\text{SSC}} = 2.4$  with  $\tau_{\text{tr}} = 2$  zs and  $\tau_{\text{SSC}} = 40$  zs. The solid, long dashed, medium dashed and short dashed lines correspond to the detected fission fragment, complementary fission fragment, CN and total contribution, respectively.

channel due to its low multiplicity. We have included the GDR  $\gamma$ -ray emission as a competing channel in the code. The GDR  $\gamma$ -ray emission width ( $\Gamma_\gamma$ ) and decay rate ( $R_\gamma d\epsilon_\gamma$ ) [33,34] according to the standard statistical model are

$$R_\gamma \epsilon_\gamma = \frac{\Gamma_\gamma(\epsilon_\gamma)}{\hbar} = \frac{\rho(E_f, J_f, \pi_f)}{2\pi \hbar \rho(E_i, J_i, \pi_i)} f_{\text{GDR}}(\epsilon_\gamma), \quad (1)$$

where  $E_f = E_i - \epsilon_\gamma$  and  $f_{\text{GDR}}(\epsilon_\gamma)$  is the GDR strength function given as [10,34]

$$f_{\text{GDR}}(\epsilon_\gamma) = 2.09 \times 10^{-5} \frac{NZ}{A} S \frac{\Gamma_{\text{GDR}} \epsilon_\gamma^4}{(\epsilon_\gamma^2 - E_{\text{GDR}}^2)^2 + \Gamma_{\text{GDR}}^2 \epsilon_\gamma^2}. \quad (2)$$

Here,  $S$  is the fraction of the classical Thomas–Reiche–Kuhn sum rule which is exhausted by the resonance.  $N$ ,  $Z$  and  $A$  are the neutron, proton and mass number, respectively of the nucleus, and  $E_{\text{GDR}}$  and  $\Gamma_{\text{GDR}}$  are the energy and width of the GDR built on the state  $(E_f, J_f)$ . The function  $f_{\text{GDR}}(\epsilon_\gamma)$  is dimensionless and all the energies are in MeV.

Equation (1) was used to calculate the  $\gamma$  decay width and included in JOANNE2. The fissioning nuclei were considered as axially-symmetric spheroids. The required GDR strength function was calculated using eq. (2) in a separate program and the output is written to a file. For both pre-saddle and saddle-to-scission regions, the strength functions were calculated by providing  $Z$ ,  $A$ , temperature, angular momentum, elongation and neck radius of the fissioning nuclei as inputs. The temperature of the CN in the pre-saddle region was taken as 1.95 MeV (same as the value used for neutron multiplicity data analysis). In the post-saddle region the temperature was 1.8 MeV. The angular momentum of the CN was taken as  $36\hbar$ . The mean pre-saddle deformation was also fixed as 1.31. All these values are the same as the ones used in the analysis of neutron and light charged particle data. Saddle-to-scission deformation was varied to reproduce the high-energy part of the GDR  $\gamma$ -ray multiplicity spectra.

The mean angular momentum of fission fragments was calculated using the formula [35]  $I_{\text{FF}} = \frac{1}{2} \{ \frac{2}{7} I_{\text{CN}} + 18 - 0.17 I_{\text{CN}} \}$ . The fragment temperature was calculated to be 1.2 MeV. Many simplifying assumptions were made while calculating the emission of  $\gamma$ -rays from fission fragments. The fission fragments were assumed to be spherical. Only the  $E1$  mode of  $\gamma$  decay was considered from the fission fragments. Instead of the mass and charge distributions, average mass and charge were used.

The folded spectra from all the three components calculated using JOANNE2 were added and compared with the experimental spectra. Figures 3 and 4 show the experimental data along with the three components and the added spectra for  $Z_{\text{ssc}} = 2.4$  and 1.8, respectively. All the other statistical model parameters were taken from the analysis of neutron and light charged particle multiplicity data.  $\tau_{\text{tr}} = 2$  zs and  $\tau_{\text{ssc}} = 40$  zs were used in the analysis. A 100% sum rule strength was used for pre-scission component. For fission fragments the sum rule strength was suitably adjusted to fit the data. As can be seen from the figure, the higher energy part of the spectrum is explained better by  $Z_{\text{ssc}} = 2.4$ . Due to the simplicity of assumptions made regarding the emission from fission fragments, the low-energy part is not reproduced very well. The focus of the present work is in fission time-scales and for this the higher energy region (where emission from the fragments is very small) is more relevant. Our analysis indicates that the information

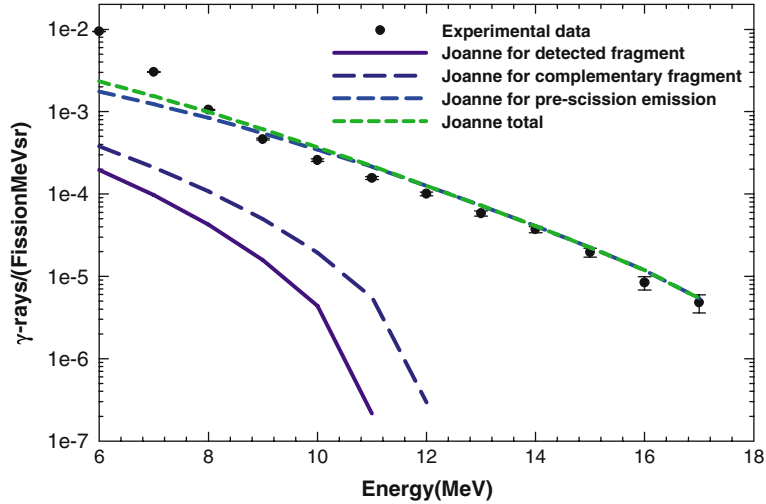


Figure 4. Same as figure 3 for  $Z_{\text{ssc}} = 1.8$ .

deduced from GDR  $\gamma$ -ray multiplicity data is consistent with those obtained from neutron, proton and  $\alpha$  particle multiplicity data as far as the fission time-scale is considered. Hence it can be concluded that pre-saddle lifetimes ( $\tau_{\text{tr}}$ ) are in the range of 0–2 zs, saddle-to-scission lifetimes ( $\tau_{\text{ssc}}$ ) are around 36–39 zs and the total lifetime ( $\tau_{\text{tot}}$ ) is in the range of 36–41 zs for nuclei in this mass region having temperature, angular momentum and isospin which are close to the one populated in the experiment.

#### 4. Summary and conclusion

For the first time, pre-scission neutron, light charged particle and GDR  $\gamma$ -ray multiplicities were measured simultaneously for  $^{28}\text{Si}+^{175}\text{Lu}$  at 159 MeV. These multiplicities were reproduced using the code JOANNE2 and fission time-scales were obtained. The calculations took into account the effect of deformation on available excitation energies, particle binding energies, charged particle transmission coefficients and level densities. The results hint at emission of neutrons closer to scission and emission of charged particles closer to saddle. The GDR  $\gamma$ -ray multiplicity data are also explained well with  $\tau_{\text{tr}} = 2$  zs and  $\tau_{\text{ssc}} = 40$  zs if we assume that the GDR  $\gamma$ -ray is emitted close to the scission point.

#### 5. Future directions

It will be interesting to measure the fission time-scale using both direct and indirect methods simultaneously. Langevin dynamics calculation to reproduce all the results simultaneously using the same parameter set can shed more light towards understanding these discrepancies.

## Acknowledgements

The authors thank A Mitra and S K Rathi for their valuable help and S S Kapoor for his suggestions. The authors also thank the LINAC-Pelletron accelerator facility staff for the smooth operation of the accelerator and A B Parui, H H Oza and R P Vind for their help during the experiment.

## References

- [1] K Ramachandran, A Chatterjee, A Navin, K Mahata, A Shrivastava, V Tripathi, S Kailas, V Nanal, R G Pillay, A Saxena, R G Thomas, Suresh Kumar and P K Sahu, *Phys. Rev. C* **73**, 064609 (2006)
- [2] K Ramachandran, *Fission time-scales from pre-scission multiplicities and evaporation residue cross-sections*, Ph.D. thesis (The University of Mumbai, 2011)
- [3] V Singh et al, *Phys. Rev. C* **87**, 064601 (2013)
- [4] R Sandal et al, *Phys. Rev. C* **87**, 014604 (2013)
- [5] D Jacquet and M Morjean, *Prog. Part. Nucl. Phys.* **63**, 155 (2009)
- [6] R P Schmitt et al, *Phys. At. Nuclei* **66**, 1163 (2003)
- [7] A Saxena et al, *Nucl. Phys. A* **730**, 299 (2004)
- [8] A Chatterjee, A Navin, S Kailas, P Singh, D C Biswas, A Karnik and S S Kapoor, *Phys. Rev. C* **52**, 3167 (1995)
- [9] H Ikezoe, Y Nagame, I Nishinaka, Y Sugiyama, Y Tomita, K Ideno, S Hamada, N Shikazono, A Iwamoto and T Ohtsuki, *Phys. Rev. C* **49**, 968 (1994)
- [10] Peter Paul and Michael Thoennessen, *Annu. Rev. Nucl. Part. Sci.* **44**, 65 (1994)
- [11] J P Lestone, *Phys. Rev. Lett.* **70**, 2245 (1993)
- [12] D J Hinde, *Nucl. Phys. A* **553**, 255c (1993)
- [13] D J Hinde, D Hilscher, H Rossner, B Gebauer, M Lehmann and M Wilpert, *Phys. Rev. C* **45**, 1229 (1992)
- [14] J U Andersen et al, *Phys. Rev. Lett.* **99**, 162502 (2007)
- [15] M O Frégeau et al, *Phys. Rev. Lett.* **108**, 122701 (2012)
- [16] J P Lestone, J R Leigh, J O Newton, D J Hinde, J X Wei, J X Chen, S Elfstrom and M Zielinska-Pfabe, *Nucl. Phys. A* **559**, 277 (1993)
- [17] B B Back, D J Blumenthal, C N Davids, D J Henderson, R Hermann, D J Hofman, C L Jiang, H T Penttila and A H Wuosmaa, *Phys. Rev. C* **60**, 044602 (1999)
- [18] J Cabrera et al, *Phys. Rev. C* **68**, 034613 (2003)
- [19] V Tishchenko, C-M Herbach, D Hilscher, U Jahnke, J Galin, F Goldenbaum, A Letourneau and W-U Schroder, *Phys. Rev. Lett.* **95**, 162701 (2005)
- [20] B Lott et al, *Phys. Rev. C* **63**, 034616 (2001)
- [21] H Ikezoe, N Shikazono, Y Nagame, Y Sigiya, Y Tomita, K Ideno, I Nishinaka, B J Qi, H J Kim, A Iwamoto and T Ohtsuki, *Phys. Rev. C* **46**, 1922 (1992)
- [22] V A Drozdov, D O Eremenko, O V Fotina, G Giardina, F Malaguti, S Yu Platonov, A F Tulinov, A Uguzzoni and O A Yuminov, *Nucl. Instrum. Methods: Phys. Res. B* **230**, 589 (2005)
- [23] F Goldenbaum et al, *Phys. Rev. Lett.* **82**, 5012 (1999)
- [24] M Morjean et al, *Nucl. Phys. A* **630**, 200c (1998)
- [25] J D Molitoris et al, *Phys. Rev. Lett.* **70**, 537 (1993)
- [26] Y Aritomoa, M Ohtab, T Maternac, F Hanappec, O Dorvauxd and L Stuttged, *Nucl. Phys. A* **759**, 309 (2005)
- [27] Gargi Chaudhuri and Santanu Pal, *Phys. Rev. C* **65**, 054612 (2002)
- [28] J Toke and W J Swiatecki, *Nucl. Phys. A* **372**, 141 (1981)

- [29] K Mahata, S Kailas, A Shrivastava, A Chatterjee, P Singh, S Santra and B S Tomar, *Phys. Rev. C* **65**, 034613 (2002)
- [30] Arnold J Sierk, *Phys. Rev. C* **33**, 2039 (1986)
- [31] S K Rathi, S Kumar, E T Mirgule, H H Oza, A Mitra, V M Datar and D R Chakrabarty, *Nucl. Instrum. Methods: Phys. Res. A* **482**, 355 (2002)
- [32] W Nelson, H Hirayama and D Roger, in: Stanford University Report SLAC (1985), p. 265
- [33] F Puhlhofer, *Nucl. Phys. A* **280**, 267 (1977)
- [34] D R Chakrabarty, S Sen, M Thoennessen, N Alamanos, P Paul, R Schicker, J Stachel and J J Gaardhoje, *Phys. Rev. C* **36**, 1886 (1987)
- [35] J J Gaardhoje, *Annu. Rev. Nucl. Part. Sci.* **42**, 483 (1992)